

# Predictions of highest Transition-temperature for electron-phonon superconductors

Wei Fan <sup>\*,1</sup>

*Key Laboratory of Materials Physics, Institute of Solid State Physics, Chinese  
Academy of Sciences, 230031-Hefei, People's Republic of China*

---

## Abstract

Using the Eliashberg strong coupling theory with vertex correction, we calculate maps of transition temperatures ( $T_c$ ) of electron-phonon superconductors in full parameter space. The maximums of transition temperatures for superconductors are predicted based on the maps and the criterion of instability of superconductivity. The strong vertex correction and high transition temperature are tightly correlated in superconductors. We predict that the maximum of  $T_c$  of new iron-based superconductors will be close to 90(K).

*Key words:*  $T_c$  Map, Vertex correction, Eliashberg-Nambu Theory

*PACS:* 74.20.Fg, 74.20.-z

---

## 1 Introductions

The researches to find home-temperature superconductors are still highlight in the field of material science [1]. The theoretical predictions of  $T_c$  are the main efforts of theoretical scientists working in this field. The BCS theory [2] and Eliashberg strong coupling theory [3–7] are well known acceptable theories to explain the superconductivity of electron-phonon superconductors. There exists the well known upper limit of  $T_c$  defined by the McMillan  $T_c$  formula [7]. The lattice instability (softening phonon) and the total strength of electron-phonon coupling also set the bounds of  $T_c$  of electron-phonon superconductors [8]. The dielectric properties have been expected to have significant influence on the possible maximum of  $T_c$  for a variety of superconductors, but

---

\* Corresponding Author : Wei Fan

*Email address:* fan@theory.issp.ac.cn (Wei Fan ).

<sup>1</sup> Tel : 0086-0551-5591-464; Fax : 0086-0551-5591-434

the problem is still not answered because the complex relation between effective electron-electron interaction and dielectric function [9]. The magnetic fluctuation and the vertex correction (non-adiabatic effects) [10] can suppress the  $T_c$  and lead to the instability of superconductivity of electron-phonon superconductors. .

The new novel Iron-based high-temperature superconductor [11–15] has been discovered and the new record of transition temperature  $T_c$  has reached about 57.4 (K) by doping rare earth elements into CaFeAsF [15]. Especially the significant normal isotope effects of iron with  $\alpha \sim 0.4$  for  $\text{Ba}_{1-x}\text{K}_x\text{Fe}_2\text{As}_2$  indicates that electron-phonon interaction plays an essential role to explain their superconductivity [16]. The Eliashberg theory suitable for both weak-coupling and strong-coupling should be studied in more detailed. It is very desirable to study the effects of vertex correction beyond Migdal theorem [10], especially for superconductors have components of light atoms. The Eliashberg theory has been successfully used to calculate  $T_c$  of many types of superconductors [17–19]. However, only special regions in parameter space of  $\lambda - \Omega_P - \mu^*$  have been explored, where  $\lambda$  is the parameter of electron-phonon interaction,  $\Omega_P$  the frequency of phonon and  $\mu^*$  the Coulomb pseudo-potential. In this paper, we present the information (  $T_c$  map ) in full parameter space  $\lambda - \Omega_P - \mu^*$ . The  $T_c$  maps obtained in this paper are very helpful to analyze the relation between  $T_c$  and these superconducting parameters and guide to find the superconductors with higher  $T_c$ .

## 2 Theory

In the paper, we generalize the equation of energy gap in reference [10] by including the Coulomb interaction. The standard energy-gap equation with the form of imaginary Matsubara's formulation [5] and the equation after having considered vertex corrections are used in our calculations. For isotropic electron-phonon interaction,

$$H_{ep} = J \sum_{\alpha,pq} c_{\alpha,p}^+ c_{\alpha,p+q} (a_{\alpha,-q}^+ + a_{\alpha,q}), \quad (1)$$

the calculations of vertex corrections are greatly simplified. The electron-phonon interactions are included in the vertex corrections only by the functions of electron-phonon interaction  $\lambda(n)$  defined below. The self-energy and Green's function of electron in the Nambu scheme are expressed as

$$\begin{aligned} \hat{\Sigma}(k, i\omega_n) &= (1 - Z(k, i\omega_n))i\omega_n \hat{\tau}_0 - \phi(k, i\omega_n) \hat{\tau}_1 + \chi(k, i\omega_n) \hat{\tau}_3, \\ \hat{G}(k, i\omega_n) &= \frac{i\omega_n Z(k, i\omega_n) \hat{\tau}_0 - \phi(k, i\omega_n) \hat{\tau}_1 + \varepsilon_k(i\omega_n) \hat{\tau}_3}{(i\omega_n)^2 Z^2(k, i\omega_n) - \varepsilon_k^2(i\omega_n) - \phi^2(k, i\omega_n)}, \end{aligned} \quad (2)$$

where  $\phi(k, i\omega_n)$  is the function of energy gap,  $Z(k, i\omega_n)$  the renormalization function, and  $\varepsilon_k(i\omega_n) = \varepsilon_k^0(i\omega_n) + \chi(k, i\omega_n)$ . In above equations  $\hat{\tau}_1$  and  $\hat{\tau}_3$  are two Pauli matrixes and  $\hat{\tau}_0$   $2 \times 2$  unity matrix.

If the density of state of phonon  $F(\nu) = V/(2\pi)^d \int d^d p B(p, \nu)$  and its spectral function  $B(p, \nu)$  are known, the effective electron-phonon interaction  $\alpha^2(\nu)$  is defined by

$$\alpha^2(\nu)F(\nu) = \frac{V}{W} \int_S \frac{d^{d-1}p}{v_F} \int_{S'} \frac{d^{d-1}p'}{v_{F'}} B(p - p', \nu) |J_{p-p'}^e|^2, \quad (3)$$

where  $W = (2\pi)^d \int_S d^{d-1}p/v_F$ ,  $v_F$  Fermi velocity and  $J_{p-p'}^e$  the matrix element of electron-phonon interaction which is constant  $J$  in this work. The first order self-energies of electrons contributed from electron-phonon interaction and electron-electron interaction are standard and written as

$$\begin{aligned} \hat{\Sigma}^1(i\omega_n) &= k_B T \sum_{n'} \lambda(n - n') \int_{-E_F}^{E_F} d\varepsilon_{k'} \hat{\tau}_3 \hat{G}(\varepsilon_{k'}, i\omega_{n'}) \hat{\tau}_3 \\ \hat{\Sigma}^e(i\omega_n) &= -k_B T \sum_{n'} \mu^* \int_{-E_F}^{E_F} d\varepsilon_{k'} \hat{\tau}_3 \hat{G}^{od}(\varepsilon_{k'}, i\omega_{n'}) \hat{\tau}_3 \end{aligned} \quad (4)$$

where  $\hat{G}^{od}(\varepsilon_{k'}, i\omega_{n'})$  is off-diagonal part of Green's function matrix  $\hat{G}(\varepsilon_{k'}, i\omega_{n'})$ . For convenience, the kinetic energy  $\varepsilon_{k'}$  has to shift  $\varepsilon_{k'} - E_F$  and a symmetric band from  $-E_F$  to  $E_F$  is chosen. Additionally we assume  $k'$ -dependent  $\hat{G}(k', i\omega_{n'})$  realized by  $\hat{G}(\varepsilon_{k'}, i\omega_{n'})$ . The electron-phonon interaction is included in  $\lambda(n) = 2 \int_0^\infty d\nu \alpha^2 F(\nu) \nu / (\nu^2 + \omega_n^2)$ . The Coulomb pseudo-potential is defined as  $\mu^* = \mu_0 / (1 + \mu_0 \ln(E_F/\omega_0))$ , where  $\mu_0 = N(E_F)U$ ,  $N(E_F)$  the density of state at Fermi energy  $E_F$ ,  $U$  the Coulomb interaction between electrons and  $\omega_0$  characteristic energy of typical phonon correlated to superconductivity.

The lowest order vertex correction comes from the second order self-energy that is written as

$$\begin{aligned} \hat{\Sigma}^2(k, i\omega_n) &= (k_B T)^2 |J|^4 \sum_{n'n''k''} D(k - k', i\nu_{n-n'}) D(k - k'', i\nu_{n-n''}) \\ &\quad \times \hat{\tau}_3 \hat{G}(k', i\omega_{n'}) \hat{\tau}_3 \hat{G}(k''', i\omega_{n'''}) \hat{\tau}_3 \hat{G}(k'', i\omega_{n''}) \hat{\tau}_3 \end{aligned} \quad (5)$$

where  $D(k^*, i\nu_{n^*})$  is phonon Green's function with the definitions of indexes  $n^* = n - n'$  or  $n - n''$ ,  $n''' = n' + n'' - n$ ,  $k^* = k - k'$  or  $k - k''$  and  $k''' = k' + k'' - k$ . The summation  $\sum_{k^*}$  of wave vector  $k^*$  ( $k^* = k'$  or  $k''$ ) is replaced by  $V/(2\pi)^3 \int d^3 k^* = V/v_F (2\pi)^3 \int d^2 k^* \int d\varepsilon_{k^*}$ . We introduce an integral  $(1/2E_F) \int_{-E_F}^{E_F} d\varepsilon_{k''}$  in Eq.(5). So the second order self-energy after having averaged on Fermi surface can be simplified as

$$\begin{aligned}
\hat{\Sigma}^2(i\omega_n) &= \frac{(k_B T)^2}{2E_F} \Sigma_{n'n''} \lambda(n-n') \lambda(n-n'') \\
&\times \int_{-E_F}^{E_F} d\varepsilon_{k'} \int_{-E_F}^{E_F} d\varepsilon_{k''} \int_{-E_F}^{E_F} d\varepsilon_{k'''} \\
&\times \hat{\tau}_3 \hat{G}(\varepsilon_{k'}, i\omega_{n'}) \hat{\tau}_3 \hat{G}(\varepsilon_{k''}, i\omega_{n''}) \hat{\tau}_3 \hat{G}(\varepsilon_{k'''}, i\omega_{n'''}) \hat{\tau}_3
\end{aligned} \tag{6}$$

now  $\varepsilon_{k''}$  is an independent variable. Three integrals of kinetic energy can independently be done by

$$\int_{-E^*}^{E^*} d\varepsilon_{k^*} \hat{G}(\varepsilon_{k^*}, i\omega_n) = -\pi (i s_n \tau_0 + \frac{\Delta_n}{|\omega_n|} \tau_1) a_n \tag{7}$$

when temperature is very close to  $T_c$ ,  $\phi(k, i\omega_n) \rightarrow 0$ , so we ignore the term  $\phi^2(k, i\omega_n)$  in the denominator of Green's function Eq.(2). Other parameters are defined as  $s_n = \omega_n/|\omega_n|$ ,  $a_n = (2/\pi) \arctan(E^*/|\omega_n|)$  and  $\Delta_n = \phi(i\omega_n)/Z(i\omega_n)$  the energy-gap parameter. In the general situation, the second-order self-energy cannot simply be written as the functions of  $\lambda(n)$ . In terms of above approximation, we transform the formulas of second-order self energy to a new formation which is suitable for numerical calculations. Although effects of electron-electron correlation are not treated accurately, the above approximation is still reasonable because the main contributions to superconductivity come from  $\lambda(n-n')\lambda(n-n'')$  in Eq.(5) and Eq.(6).

The total self-energy we consider is  $\Sigma(i\omega_n) = \Sigma^1(i\omega_n) + \Sigma^c(i\omega_n) + \Sigma^2(i\omega_n)$ . By combining with Dyson Equation and considering that, when temperature is very close to  $T_c$ ,  $\Delta_n \rightarrow 0$ , the terms proportional to  $\Delta^2$  are ignored and the energy-gap equation is generalized to

$$\sum_{n'=-\infty}^{+\infty} (K_{nn'} - \rho \delta_{nn'}) \frac{\Delta_{n'}}{|\omega_{n'}|} = 0, \tag{8}$$

where the kernel matrix

$$\begin{aligned}
K_{nn'} &= [\lambda(n-n')B(nn') - \mu^* + C(nn')]a_{n'} - \delta_{nn'}H_{n'}, \\
H_{n'} &= \sum_{n''=-\infty}^{+\infty} [\delta_{n'n''} \frac{|\omega_{n''}|}{\pi k_B T} + \lambda(n'-n'')A(n'n'')s_{n'}s_{n''}a_{n''}]
\end{aligned} \tag{9}$$

with parameters  $A(nn') = 1 - V_A(nn')$ ,  $B(nn') = 1 - V_B(nn')$  and  $a_n = (2/\pi) \arctan(E_F/Z_n|\omega_n|)$ . The 3-dimensional parameters of vertex correction have the form

$$\begin{aligned}
V_A(nn') &= (\pi^2 k_B T / 2E_F) \sum_{n''} \lambda(n - n'') s_{n'+n''-n} s_{n''} a_{n'+n''-n} a_{n''} \\
V_B(nn') &= (\pi^2 k_B T / E_F) \sum_{n''} \lambda(n - n'') s_{n'+n''-n} s_{n''} a_{n'+n''-n} a_{n''} \\
C(nn') &= (\pi^2 k_B T / 2E_F) \sum_{n''} \lambda(n - n'') \lambda(n' - n'') s_{n'-n''+n} s_{n''} a_{n'-n''+n} a_{n''}.
\end{aligned} \tag{10}$$

If we ignore the vertex corrections, three parameters  $V_A(nn')$ ,  $V_B(nn')$  and  $C(nn')$  are all equal to zero and the kernel Eq.(9) of energy-gap equation reduces to the general form without vertex correction [5]. At the same time, the differences of the equations of energy gap in 3-dimensional and 2-dimensional space are only included in the function  $\alpha^2 F(\nu)$  if vertex corrections are ignored. The introduction of pair-breaking parameter  $\rho$  creates an eigenvalue problem. The physical gap-equation is corresponding to  $\rho=0$ . In the calculation of  $a_n$ , we choose  $Z_n \sim 1$  the value of normal state. The  $T_c$  is defined as the temperature when the maximum of eigenvalues  $E^{max}$  of kernel matrix  $K_{nn'}$  crosses zero and changes its sign. We use about  $N=200$  Matsubara's energies to solve above equation. The method to find  $T_c$  is similar to the bisection method used to find the roots of a nonlinear equation [20]. The nonlinear equation to find  $T_c$  is  $E^{max}(T)=0$ . We can reach the accurate of 0.0001(K) after only 20-30 iterations in temperature interval from 0 (K) to 600 (K).

In calculations of  $\alpha^2 F(\nu)$ , we assume that  $\alpha^2(\nu)$  is approximately a constant around the peak of phonon mode and the density of state of phonon is expressed as

$$F(\nu) = \begin{cases} \frac{c}{(\nu - \Omega_P)^2 + (\omega_2)^2} - \frac{c}{(\omega_3)^2 + (\omega_2)^2}, & |\nu - \Omega_P| < \omega_3 \\ 0 & \text{others,} \end{cases} \tag{11}$$

where  $\Omega_P$  is the energy of phonon mode,  $\omega_2$  the half-width of peak of phonon mode and  $\omega_3 = 2\omega_2$ . The parameter of electron-phonon interaction is defined as  $\lambda = \lambda(0) = 2 \int_0^\infty d\nu \alpha^2 F(\nu) / \nu$ . An important relation

$$M \langle \nu^2 \rangle \lambda = \eta = const \tag{12}$$

will be used, where  $M$  is the effective mass for a certain phonon mode, especially the constant  $\eta$ , the so-called McMillan-Hopfield parameter, is closely related to  $T_c$  [5]. The superconductor parameter  $\eta = N(E_F) \langle J^2 \rangle$ , characterizes the chemical environment of atoms and almost keeps as a constant against the simple structural changes or isotope substitutions.

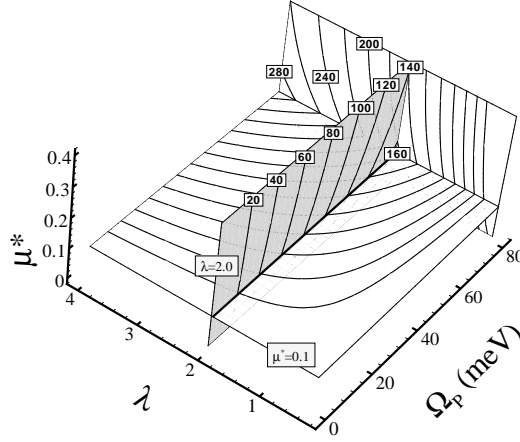


Fig. 1. The 3-dimensional  $T_c$  map and three slice planes with  $\lambda=2.0$ ,  $\mu^*=0.1$  and  $\Omega_P=80$  meV. The numbers within the rectangles nearby the contour lines are  $T_c$  values of the corresponding contour lines.

### 3 $T_c$ Map without vertex corrections

A  $T_c$  map in full parameter-space  $\lambda - \Omega_P - \mu^*$  is very helpful to understand the superconductivity with electron-phonon mechanism. At first, we choose three-dimensional  $30 \times 30 \times 30$  mesh-grid with  $0.4 \leq \lambda \leq 4.0$ ,  $0 \leq \mu^* \leq 0.4$  and  $5.0 \text{ meV} \leq \Omega_P \leq 80 \text{ meV}$ . We calculate  $T_c$  on every mesh point using Eq.(8). We plot three slice planes with  $\lambda=2.0$ ,  $\mu^*=0.1$  and  $\Omega_P=80$  meV respectively shown in Fig.1. Comparing with others two parameters, the choice of  $\mu^*$  has smaller effects on  $T_c$ . The parameter  $\lambda=2.0$  is the upper limit of electron-phonon interaction [7]. When the parameter  $\lambda$  is larger than 2.0, the crystal lattice will be unstable. In our calculations, the half-height width  $\omega_2$  has the same value (4 meV) for all points of the  $T_c$  map. If the peak of phonon mode is not too broad, the  $T_c$  map has no significant change. Conversely, the Einstein mode with  $\omega_2 \sim 0$  has higher  $T_c$ .

In Fig.2, we plot a  $T_c$  map in two-dimensional  $\lambda - \Omega_P$  plane in details using  $50 \times 100$  mesh-grid with parameters  $\lambda$  from 0.4 to 4.0,  $\Omega_P$  from 5 meV to 160 meV and the Coulomb pseudo-potential  $\mu^*=0.1$ . The two-dimensional map is the extension of the slice of the corresponding 3-dimensional map with  $\mu^*=0.1$  shown in Fig.1. The important role of the relation  $M\langle\nu^2\rangle\lambda=\text{const}$  of Eq.(12) can be shown clearly on the  $T_c$  map. If the effective mass  $M$  of a certain phonon mode is constant, so is the parameter  $\langle\nu^2\rangle\lambda$ . We assume the half-width of peak of phonon mode  $\omega_2 \ll \Omega_p$ , so  $\langle\nu^2\rangle\lambda \sim \Omega_p^2\lambda=\text{const}$ . The two curves of  $\Omega_p^2\lambda=320$  and  $3600 \text{ (meV)}^2$  are plotted in the same map. In the regime of strong coupling,  $k_B T_c$  is approximately equal to  $a\sqrt{\langle\nu^2\rangle\lambda}$

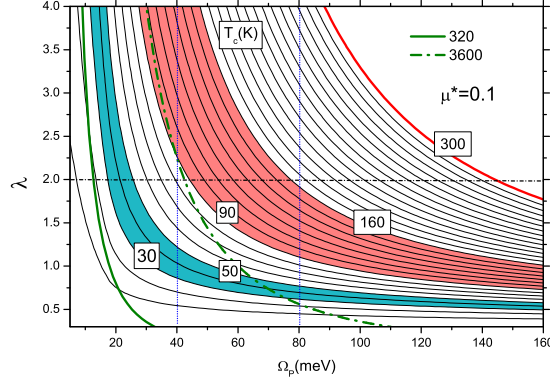


Fig. 2. The  $T_c$  map in  $\lambda - \Omega_p$  plane with  $\mu^*=0.10$  obtained from imaginary-energy Matsubara's method. The bold solid line and dash-dot line are the curves  $\lambda\Omega_p^2=320$  ( $\text{meV})^2$  ( $T_c^{\text{max}}=24$  K) and  $3600$  ( $\text{meV})^2$  ( $T_c^{\text{max}}=80$  K) respectively.

$\sim a\sqrt{\Omega_p^2\lambda}$ , where  $a=0.115$ . Thus  $\langle\nu^2\rangle\lambda=\text{const}$  is equivalent to  $T_c=\text{const}$ . In fact,  $\langle\nu^2\rangle\lambda=\text{const}$  was used to define the possible maximum of  $T_c$  [7]. The  $T_c$  increases with  $\lambda$  and saturates at  $\lambda = 2$  by using the McMillan formula. Similar to McMillan's idea, our results in the Fig.2 just show that the two curves coincide approximately with the contour lines of  $T_c$  in strong-coupling regime. The approximate saturations happen when  $\lambda$  is very close to 2.

The term  $\langle\nu^2\rangle\lambda$  characterizes the possible maximum of  $T_c$  for fixed  $\langle\nu^2\rangle\lambda$  value if we consider possible bounds on  $\lambda$ . We can see from the Fig.2 that the curve will have more chances to meet contour lines with higher  $T_c$  for larger  $\langle\nu^2\rangle\lambda$ . Thus, the maximums of  $T_c$  above two curves with  $\Omega_p^2\lambda=320, 3600$  ( $\text{meV})^2$  are close to 20K and 80K respectively. When superconductor under small structural modifications or isotope substitution, the corresponding parameters  $\lambda$  and  $\Omega_p$  move along these curves because the chemical environments keep almost unchanged. In the region of high-energy phonon, the smaller change of  $\lambda$  can induce larger change of  $T_c$  because the curve  $\Omega_p^2\lambda=3600$  ( $\text{meV})^2$  spans more contour-lines.

To study effects of Coulomb pseudo-potential  $\mu^*$ , we calculate two others  $T_c$  maps in  $\mu^* - \lambda$  plane with mesh-grid  $50\times 50$  for two phonon energies  $\Omega_p=10$  meV and 40 meV respectively (Fig.3). For  $\Omega_p=10$  meV, the maximum of  $T_c$  is about 24 K, however 100 K for  $\Omega_p=40$  meV. We can find that when  $\mu^* > 0.2$ ,  $\mu^*$  have smaller influences on  $T_c$ .

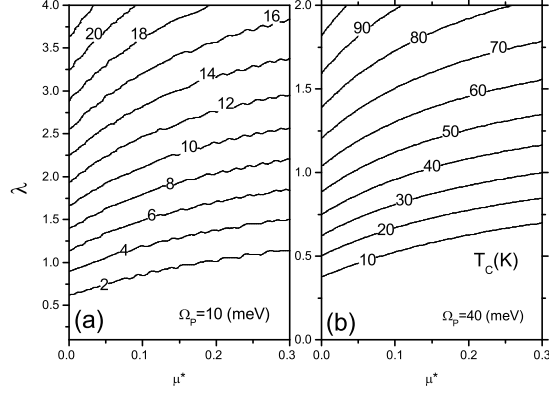


Fig. 3.  $T_c$  maps in  $\mu^* - \lambda$  plane with  $\Omega_P=10$  meV (a) and 40 meV (b).

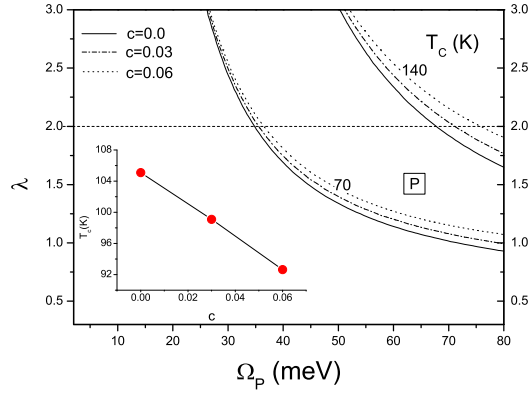


Fig. 4. The effects of vertex correlations on  $T_c$  map ( $\mu^*=0.10$ ) with two parameters  $c=0.12(\text{eV})/E_F=0.03$  and  $0.06$  compared with the results without vertex corrections  $c=0.0$  ( $E_F = \infty$ ). Two groups of contour lines with  $T_c=70\text{K}$  and  $140\text{K}$  are plotted for three values of  $c=0.0, 0.03$  and  $0.06$  respectively. The inserted figure plots the curve of  $T_c$  by  $c$  at a fixed point  $P$  shown on the  $\lambda - \Omega_P$  plane.

#### 4 $T_c$ Map with vertex corrections

It is very important to study the vertex correction in general strong coupling theory [10]. We control the vertex correction by changing the Fermi-energy  $E_F$  in the parameter  $a_n = (2/\pi) \arctan(E_F/Z_n|\omega_n|)$ . We choose two values 1.0 eV and 2.0 eV of  $E_F$ . If  $E_F$  is too large ( $\gg 2$  eV) the vertex corrections are invisible in our calculations. Two groups of contour lines with  $T_c=70$  K and  $140$  K are plotted, and for each of groups, there are three contour lines for  $c=0.0, 0.03$  and  $0.06$  respectively, where  $c=0.12(\text{eV})/E_F$  is the control parameter of vertex correction, especially  $c=0$  or  $E_F = \infty$  is corresponding to the absence of vertex corrections. We can see that for two  $T_c$ , the vertex corrections are so small that the  $T_c$  map has no significant changes. For the same  $T_c$ , the contour lines only move to regions with larger  $\lambda$  slightly. In the

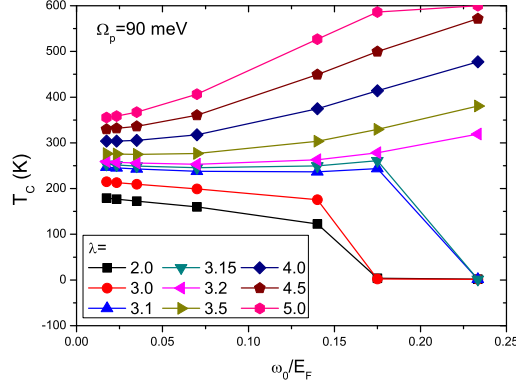


Fig. 5. The positive ( $\lambda \geq 3.2$ ) and negative vertex corrections ( $\lambda < 3.2$ ) at high phonon energy  $\Omega_P=90$  meV.

inserted figure of Fig.4, at a point  $P$  with fixed  $\lambda=1.50$  and  $\Omega_P=65$ meV, the vertex corrections decrease  $T_c$  to smaller value. However, the negative vertex corrections only happen when  $\Omega_P < 80$  meV and  $\lambda < 4$ . Beyond the ranges of parameters, such as  $\Omega_P=90$  meV and  $\lambda \geq 3.2$ , the positive vertex corrections ( $T_c$  increases with  $\omega_0/E_f$ ) are realized (Fig.5). It's not surprised that, if  $\lambda < 3.2$ , only the general negative vertex-corrections are found although the phonon energy  $\Omega_P$  is larger than 80 meV (Fig.5). The key point is that, although the effects of vertex corrections are rather complicated, they do not change the  $T_c$  maps significantly if  $E_F$  isn't too small.

We expect that the vertex corrections are strong for superconductors with high  $T_c$ . From the Fig.4, we can see that, when  $\Omega_P$  is smaller than 40 meV, the vertex effect is very small although the parameter  $\lambda$  of electron-phonon interaction is probably large. The effect of vertex correction is determined by  $\langle \nu^2 \rangle \lambda$  and not solely by the parameter  $\lambda$  of electron-phonon interaction in the region of low phonon-energy. The vertex correction is closely correlated to  $T_c$  because of  $T_c \propto \sqrt{\langle \nu^2 \rangle \lambda}$  in strong coupling regime with  $\lambda > 2.0$ . We will prove that the vertex correction is also characterized by  $\langle \nu^2 \rangle \lambda$  in the region of low phonon energy. It easily sees that the parameter  $V_A(nn') = P_V \sum_m \lambda(\nu_m) s_{n'-m} s_{n-m} a_{n'-m} a_{n-m}$  where  $P_V = \pi^2 k_B T_c / 2 E_F$  and  $m = n - n''$ . If the Einstein spectrum  $\alpha^2 F(\nu) = (\lambda/2) \Omega_P \delta(\nu - \Omega_P)$  is considered, we can get

$$\lambda(\nu_m) = \lambda \Omega_P^2 / (\nu_m^2 + \Omega_P^2). \quad (13)$$

If  $\Omega_P \rightarrow 0$ , then  $\lambda(\nu_m) \rightarrow (1/\nu_m^2) \lambda \Omega_P^2$ , and the parameter of vertex correction  $V(nn') \rightarrow P_V C(n, n', T_c) \lambda \Omega_P^2$ , where  $C(n, n', T_c) = \sum_m s_{n'-m} s_{n-m} a_{n'-m} a_{n-m} / \nu_m^2$  is well defined and finite. So the parameter  $\Omega_P^2 \lambda$  or  $\langle \nu^2 \rangle \lambda$  characterizes the vertex correction. In real materials  $\Omega_P (\ll E_F)$  has an up limit  $\Omega_D$ . When  $\Omega_P$  approaching to high energy,  $\lambda(\nu_m) \rightarrow \lambda \Omega_D^2 / (\nu_m^2 + \Omega_D^2)$ ,  $V(nn') \rightarrow P_V D(n, n', T_c) \lambda$ , where  $D(n, n', T_c) = \sum_m s_{n'-m} s_{n-m} a_{n'-m} a_{n-m} \Omega_D^2 / (\nu_m^2 + \Omega_D^2)$  is well defined.

So we can see that the vertex correction is characterized by  $\lambda$  at high energy. From the Fig.2,  $T_c$  is almost independent on  $\Omega_P$  when  $\Omega_P > 40$  meV and  $\lambda < 2.0$ , and  $T_c$  is determined by  $\lambda$  as well. Thus, we have proven that the vertex correction (as well as  $T_c$ ) is characterized by  $\langle \nu^2 \rangle \lambda$  in the region of low phonon energy and by  $\lambda$  in the region of high phonon energy. There is a characteristic energy close to 40 meV and the vertex corrections (as well as  $T_c$ ) have different behavior when  $\Omega_P$  is larger or smaller than the characteristic energy.

## 5 Discussion and Summary

For superconductors with  $T_c$  close to home temperature, the parameter  $\lambda$  of electron-phonon interaction should be larger than 2.0 or the phonon-energy  $\Omega_P$  larger than 80 meV (Fig. 2). Generally, we hope to find higher  $T_c$  by increasing the frequency of phonon by choosing compounds including light atoms such as Hydrogen atoms in molecule crystals [21]. The contour line  $T_c=300\text{K}$  in Fig.2 is beneath the line of  $\lambda=2.0$  when  $\Omega_P$  is larger than 150 meV or  $1210\text{ cm}^{-1}$  for Raman shift. We can see that only small changes of  $\lambda$  can induce large changes of  $T_c$  if  $\Omega_P > 80$  meV. In compounds with components of light atoms and heavy atoms, the frequencies of optical modes are determined by light atoms. The heavy atoms have the capability to stabilize the lattice vibrations so it is advantaged to form macroscopic-coherent superconducting states.

It is very interesting that we can explain the spatial anti-correlation between energy-gap and phonon energy of cuprate superconductor Bi2212 [22] in terms of the electron-phonon mechanism by having solved the real-energy Eliashberg Equation under the constraint from Eq.(12) [23]. The large value of  $\lambda$  ( $>1.0$ ) can be obtained from the frozen-phonon method by considering non-local long-range Madelung interaction which is non-adiabatic effect when an atom displaces away from its equilibrium position [24,25]. Our results in this context also indicate that the vertex corrections which include part of non-adiabatic effect are closely correlated to high  $T_c$ . On the other hand, in terms of the linear temperature-dependent resistivity at high temperature above  $T_c$ , the strong electron-phonon coupling could be extracted by the analysis of strong coupling theory [26,27]. The upper limit of phonon energies of in-plane breathing modes of cuprate superconductors is close to  $\Omega_P=80$  meV [28]. If the anisotropy of Bi2212 crystal is ignored, from the Fig.1, we can see that the maximum of  $T_c$  will be within 140K-160K. The highest  $T_c$  is about 130 K for cuprate superconductors close to the range. From the Fig.4, there are larger vertex corrections at higher  $\Omega_P$  and larger  $\lambda$ , however the  $T_c$  doesn't changes significantly because the band-width of  $\text{CuO}_2$  plane for cuprate superconductors such as Bi2212 is not too small about 4 eV, and the Fermi-energy  $E_F$  is at least 1 eV [29,30].

Finally, we discuss the new iron-based layered high-temperature superconductors [11–15]. The carriers are mostly possible in FeAs layers. The multi-band electronic structure, especially the cooper-pairs spanning different Fermi-surface sheets probably play an important role to its superconductivity. The pairing mechanism of different Fermi-surface sheets is absent in present model, but the model is still equivalent to the mean of multi-band model. Very similar to the cuprate superconductors, the linear-response calculation of electron-phonon interaction only provides very small parameter  $\lambda$  of electron-phonon coupling that does not account the requirement of high  $T_c$  from 27(K) to 57(K) [31]. However, just like for cuprate superconductors [25], the nonlocal long-range Madelung interaction generally enhances parameter  $\lambda$  of electron-phonon interaction and account the requirements for high  $T_c$ . Experimental evidence for strong electron-phonon coupling comes from the measurement of normal-state resistivity at high temperature [32]. The upper limit of phonon-energy is about 40 meV [33]. From the Fig.2 and Fig.3(b), we can predict that the maximum of transition temperature  $T_c$  for layered iron-based superconductors may access to 90(K).

In summary, we calculate  $T_c$  maps in full parameter space using strong coupling theory including vertex corrections. We also discuss the possibility increasing  $T_c$  by using materials including light atoms with higher phonon frequency. The strong vertex corrections are inevitable in materials with high  $T_c$ . Based on the maps obtained in this work, we predict the maximum of  $T_c$  of new finding iron-based superconductors is about 90(K).

## 6 Acknowledgement

The author gratefully thanks Dr. Li Yang-Ling for reading and criticizing the manuscript. This work is supported by Director Grants of Hefei Institutes of Physical Sciences, Knowledge Innovation Program of Chinese Academy of Sciences and National Science Foundation of China. The eigenvalues of kernel matrix are obtained by using the Lapack package.

## References

- [1] N. W. Ashcroft, *Physica C* **468** (2008) 115; W. E. Pickett, *Physica C* **468** (2008) 126; all other papers in *Room Temperature Superconductivity* edited by B. Jankó, G. W. Crabtree and W. K. Kwok, *Physica C* **468**, issue **2** (2008).
- [2] J. Bardeen, L. N. Cooper, and J. R. Schrieffer, *Phys. Rev.* **108** (1957) 1175.
- [3] G. M. Éliashberg, *Soviet. Phys. JETP*, **11** (1960) 696.

- [4] Y. Nambu, Phys. Rev. **117** (1960) 648.
- [5] P. B. Allen, and R. C. Dynes, Phys. Rev. **B 12** (1975) 905.
- [6] D. J. Scalapino, J. R. Schrieffer, and J. W. Wilkins, Phys. Rev. **148** (1966) 263.
- [7] W. L. McMillan, Phys. Rev. **167** (1968) 331.
- [8] J. E. Moussa, and M. L. Cohen, Phys. Rev. **B 74** (2006) 094520.
- [9] O. V. Dolgov, D. A. Kirzhnits, and E. G. Maksimov, Rev. Mod. Phys. **53** (1981) 81.
- [10] V. N. Kostur and B. Mitrović, Phys. Rev. **B 50** (1994) 12774.
- [11] Y. Kamihara, T. Watanabe, M. Hirano, and H. Hosono, J. AM. Chem. Soc. **130** (2008) 3296.
- [12] X. H. Chen, T. Wu, G. Wu, R. H. Liu, H. Chen, D. F. Fang, Nature 453 (2008) 761.
- [13] Z. A. Ren, J. Yang, W. Lu, W. Yi, X. L. Shen, Z. C. Li, G. C. Che, X. L. Dong, L. L. Sun, F. Zhou, Z. X. Zhao, Europhys. Lett. **82** (2008) 57002.
- [14] C. Wang, L. J. Li, S. Chi, Z. W. Zhu, Z. Ren, Y. K. Li, Y. T. Wang, X. Lin, Y. K. Luo, S. Jiang, X. F. Xu, G. H. Cao, and Z. A. Xu, Europhys. Lett. **83** (2008) 67006.
- [15] P. Cheng, B. Shen, G. Mu, X. Y. Zhu, F. Han, B. Zeng, and H. H. Wen, arXiv: 0812.1192 (2008).
- [16] R. H. Liu, T. Wu, G. Wu, H. Chen, X. F. Wang, Y. L. Xie, J. J. Yin, Y. J. Yan, Q. J. Li, B. C. Shi, W. S. Chu, Z. Y. Wu, and X. H. Chen, arXiv:0810.2694 (2008).
- [17] J. P. Carbotte, Rev. Mod. Phys. **62** (1990) 1027.
- [18] C. P. Moca, and B. Jankó, Physica **C 387** (2003) 122.
- [19] M. J. Holcomb, Phys. Rev. **B 54** (1996) 6648.
- [20] W. H. Press, S. A. Teukolsky, W. T. Vetterling and B. P. Flannery, Numerical Recipes in Fortran 77, The art of scientific computing, Second Edition, Volume **1** of Fortran Numerical Recipes, chapter 9, (Press Syndicate of the University of Cambridge, 1997).
- [21] M. I. Eremets, I. A. Trojan, S. A. Medvedev, J. S. Tse and Y. Yao, Science **319** (2008) 1506.
- [22] Jinho Lee, K. Fujita, K. McElroy, J. A. Slezak, M. Wang, Y. Aiura, H. Bando, M. Ishikado, T. Masui, Jian-Xin Zhu, A. V. Balatsky, H. Eisaki, S. Uchida, and J. C. Davis, Nature **442** (2006) 546.
- [23] W. Fan, Chinese Physics Letter, **25** (2008) 2217.

- [24] T. Jarlborg, Solid State Communications **71** (1989) 669.
- [25] H. Krakauer, W. E. Pickett, and R. E. Cohen, Phys. Rev. **B 47** (1993) 1002.
- [26] R. Zeyher, Phys. Rev. **B 44** (1991) 10404.
- [27] I. I. Mazin, O. V. Dolgov, Phys. Rev. **B 45** (1992) 2509.
- [28] G. M. Zhao, Phys. Rev. **B 75** (2007) 214507.
- [29] H. Krakauer, W. E. Pickett, Phys. Rev. Lett. **60** (1988) 1665.
- [30] H. Lin, S. Sahrakorpi, R. S. Markiewicz, and A. Bansil, Phys. Rev. Lett. **96** (2006) 097001.
- [31] L. Boeri, O. V. Dolgov, and A. A. Golubov, Phys. Rev. Lett. **101** (2008) 026403.
- [32] D. Bhoi, P. Mandal, and P. Choudhury, arXiv:0808.2695 (2008).
- [33] S. Higashitaniguchi, M. Seto, S. Kitao, Y. Kobayashi, M. Saito, R. Masuda, T. Mitsui, Y. Yoda, Y. Kamihara, M. Hirano, and H. Hosono, arXiv:0807.3968 (2008).